East European Journal of Physics. 1. 243-249 (2024)
DOI:10.26565/2312-4334-2024-1-20 ISSN 2312-4334

CASSON FLUID FLOW PAST A SHRINKING SURFACE WITH HEAT AND MASS TRANSFERS

Rajesh Kumar Das[a]*, Debasish Dey[b†]
[a]*Department of Mathematics, Pandit Deendayal Upadhyaya Adarsha Mahavidyalaya Amjonga, Goalpara, India-783124*
[b]*Department of Mathematics, Dibrugarh University, Dibrugarh, India-786004*
**Corresponding Author e-mail: rajeshkumardas91@gmail.com, †Co-author e-mail: debasish41092@gmail.com*
Received December 12, 2023; revised January 19, 2024; accepted January 24, 2024

In this study, we have numerically investigated the heat and mass transfers behaviour of Casson fluid flow past a porous shrinking sheet in existence of a magnetic field, thermal radiation, and suction or blowing at the surface. Applying suitable similarity transformations, the leading partial nonlinear differential equations of mass, flow, and heat transfer are converted into solvable ordinary differential equations, which can then be solved numerically with the help of the MATLAB bvp4c scheme. We have analyzed and shown graphically the implications of several non-dimensional controlling factors on the profiles of temperature, concentration, and velocity. Additionally, the Sherwood, Nusselt, and Skin friction for Casson fluids are examined and tabulated. The current study's findings for Casson fluid exhibit great consistency with previous research under specific circumstances.
Keywords: *Casson fluid; heat and mass transfers; permeability; MHD; shrinking sheet*
PACS: 44.05.+e

1. INTRODUCTION

There are numerous uses for the study of non-Newtonian fluids in industries and engineering, particularly in the process of separating fossil oil from petroleum goods. A Casson fluid is a non-Newtonian fluid with yield stress. Additionally, due to the chain structure of blood cells and the materials they carry, such as protein, fibrinogen, rouleaux, etc., human blood may also be considered a Casson fluid. Thus, the Casson fluid plays a significant role in both biological science and engineering. The problem of the flow by reason of stretching or shrinking sheets has attracted many researchers, and it is a topic of attention in the literature (Grubka and Bobby [1], Banks [2], Crane [3], Keller and Magyari [4], Lio and Pop [5], etc.). Boundary layer flows have many significant applications in industrial manufacturing processes. Though there aren't enough works on the flow past on shrinking sheets, Wang [6] was the foremost to study the unstable viscous flow caused by a shrinking sheet. Mikalavcic and Wang [7] have examined the viscous hydrodynamic flow caused by the shrinking surface for particular values of the suction parameter and came to the conclusion that, for both two-dimensional and axi-symmetric flows, the shrinking sheet solution might not be unique at particular suction rates. After that, Fang and Zhang [8] have clarified how an external magnetic field affects the flow of a shrinking sheet and discovered that a high magnetic field ensures a constant flow of the boundary layer. Following that, several scholars [9–21] examine the non-Newtonian fluid flow past a diminishing sheet from a variety of physical angles.

On the contrary, Hayat *et al.* [22–24] have examined non-Newtonian fluid flow over a shrinking surface. Since most fluids encountered in scientific processes exhibit non-Newtonian fluid characteristics [25–31], research on non-Newtonian flows is important from a technological standpoint. Notable studies on the non-Newtonian fluid flow over a shrinking surface were published by Rosali *et al.* [32], Yacob *et al.* [33, 34], and Ishak *et al.* [35, 36].

Dey *et al.* [37] explored the stability of MHD Casson fluid over a porous elongating sheet. Bhattacharyya *et al.* [38] studied the MHD Casson fluid over a porous stretching/shrinking surface in the existence of wall mass transmission. Das *et al.* [39] have studied numerically to examine the nanofluid flow in permeable media past a vertical stretching surface with heat and mass transfers.

Pramanik [40] studied the characteristics of Casson fluid heat transfer via thermal radiation and porous media. Sarkar *et al.* [41] enlightened the significance of this fluid model in various contexts and in relation to heat radiation is investigated through the use of an inclined cylindrical surface. Elucidation of the non-Newtonian Casson fluid dynamics across a rotating non-uniform surface under the influence of coriolis force was enlightened by Oke *et al*. [42]. Dey et al. [43] have investigated the energy transfer and entropy creation of hydro-magnetic stagnation point flow in micropolar fluids under uniform suction and injection.

Kinetic processes like heat and mass transmission can happen and be studied individually or together. While studying them separately is easier, in the case of diffusion and convection, both processes are modelled by comparable mathematical equations. In certain situations, such as evaporative cooling and ablation, mass transfer must be taken into account in addition to heat. Problems with combined mass and heat transfer are significant in many processes, and they have gained attention recently in the chemical industry, drying, evaporation on a water surface, and the process of connecting with thermal retrieval.

In this research paper, we have examined the heat and species concentration transmission of Casson fluid through a permeable medium past a shrinking sheet. This motion is mathematically controlled by a system of non-linear PDEs that,

Cite as: R.K. Das, D. Dey, East Eur. J. Phys. 1, 243 (2024), https://doi.org/10.26565/2312-4334-2024-1-20

with the suitable transformation, are converted into non-linear ODEs. The velocity, temperature, and concentration profiles are obtained by numerically solving this system under the proper boundary conditions. The effects of the problem's physical characteristics on these results are explored graphically and numerically using a series of figures and tables. A quick analysis can produce a model that helps explain the mechanics of physiological fluxes.

2. MATHEMATICAL FORMULATION

Consider a two-dimensional, incompressible, electrically conducting hydromagnetic Casson fluid flow over a permeable, shrinking sheet with heat and mass transfer. To scrutinize the suction and blowing processes, the wall permeability characteristics have been used. Figure 1 illustrates how the non-Newtonian fluid drenches the porous material y>0 while the flow dynamics take place in the area y<0. A magnetic field B(x) has been implemented in the flow. Following Dey *et al.* [37], the rheological equation of an incompressible and isotropic Casson fluid is as follows:

$$\tau_{ij} = \begin{cases} 2\left(\mu_\beta + \dfrac{P_y}{\sqrt{2\pi}}\right)e_{ij}, & \pi > \pi_c \\ 2\left(\mu_\beta + \dfrac{P_y}{\sqrt{2\pi_c}}\right)e_{ij}, & \pi < \pi_c \end{cases}$$

where, $\pi = e_{ij}e_{ij}$ and $e_{ij}$is the $(i,j)th$ component of deformation rate.

Considering the above assumptions, the leading equations for the projected fluidic model are given by:

$$\frac{\partial u}{\partial x} + \frac{\partial v}{\partial y} = 0 \tag{1}$$

$$u\frac{\partial u}{\partial x} + v\frac{\partial u}{\partial y} = \nu\left(1 + \frac{1}{\beta}\right)\frac{\partial^2 u}{\partial y^2} - \frac{\sigma B^2(x)}{\rho}u - \frac{\nu}{k}u \tag{2}$$

$$u\frac{\partial T}{\partial x} + v\frac{\partial T}{\partial y} = \alpha\frac{\partial^2 T}{\partial y^2} \tag{3}$$

$$u\frac{\partial C}{\partial x} + v\frac{\partial C}{\partial y} = D\frac{\partial^2 C}{\partial y^2} \tag{4}$$

The relevant boundary restrictions are

$$\begin{aligned} &u = -ax, v = V_0, T = T_0, C = C_0 \text{ at } y = 0, \\ &u \to 0, T = T_\infty, C = C_\infty \text{ as } y \to \infty \end{aligned} \tag{5}$$

where u, v denotes velocity components along x and y directions, ν stands for kinematic viscosity, β represents casson fluid parameter, σ is the electrical conductivity, ρ stands for fluid density, k is the porous medium permeability, T represents fluid temperature, α denotes thermal conductivity, C describes species concentration, D is the coefficient of mass diffusion, $V_0 > 0$ and $V_0 < 0$ are assumed as blowing and suction conditions, respectively.

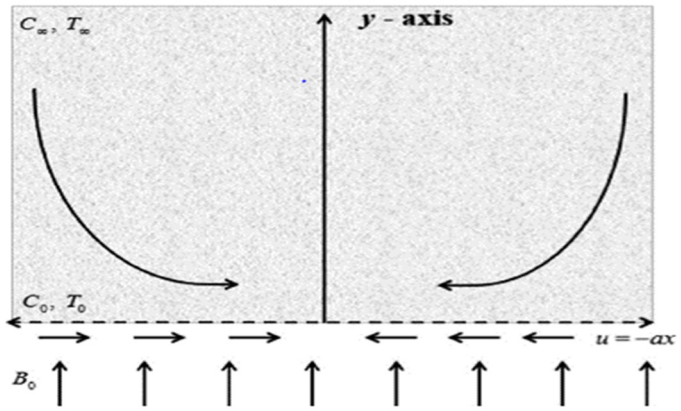

Figure 1. Flow Model

3. METHOD OF SOLUTION

Using the following similarity transformations:

$$\eta = \sqrt{\frac{a}{\nu}}y, \qquad \psi = \sqrt{a\nu}xf(\eta), \qquad \theta(\eta) = \frac{T - T_\infty}{T_0 - T_\infty}, \qquad \phi(\eta) = \frac{C - C_\infty}{C_0 - C_\infty},$$

$$M = \frac{\sigma B^2}{a\rho},\ Pr = \frac{\nu}{\alpha},\ Sc = \frac{\nu}{D},\ K_1 = \frac{\nu}{ak} \tag{6}$$

Using equation (6) in equations (2)-(5), it transforms as follows:

$$\left(1 + \frac{1}{\beta}\right) f''' + ff'' - f'^2 - M^2 f' - K_1 f' = 0 \tag{7}$$

$$\theta'' + Prf\theta' = 0 \tag{8}$$

$$\phi'' + Scf\phi' = 0 \tag{9}$$

The relevant boundary restrictions are given by

$$f(0) = S, \quad f'(0) = -1, \ \theta(0) = 1, \ \phi(0) = 1,$$
$$f'(\infty) = 0, \quad \theta(\infty) = 0, \quad \phi(\infty) = 0 \tag{10}$$

The physical parameters that are important for our studies are Sherwood number, Nusselt number, skin friction coefficient. They are expressed as

$$C_f\left(Re_x^{\frac{1}{2}}\right) = (1 + \frac{1}{\beta})f''(0), \tag{11}$$

$$Nu_x\left(Re_x^{-\frac{1}{2}}\right) = -\theta'(0), \tag{12}$$

$$Sh_x\left(Re_x^{-\frac{1}{2}}\right) = -\phi'(0), \tag{13}$$

4. RESULT AND DISCUSSION

The resultant ordinary differential equations and related surface limitations are numerically computed via the bvp4c MATLAB software. The flow behaviour patterns for diverse values of the leading parameters are displayed in both tabular and graphical form. Figure 2 exhibits the velocity profile for various values of magnetic field parameter (M). It is found that with increment in M, the magnitude of the velocity profile increase. This is because, with increment of M will dominate the Lorentz force and lessen the impact of the fluid's viscosity at the surface, increasing the fluid's speed.

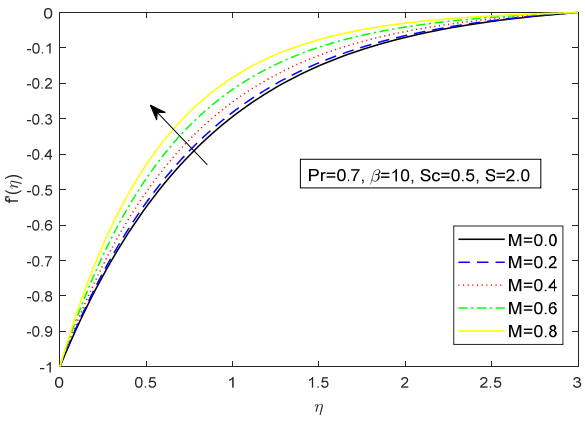

Figure 2. Velocity profile for M

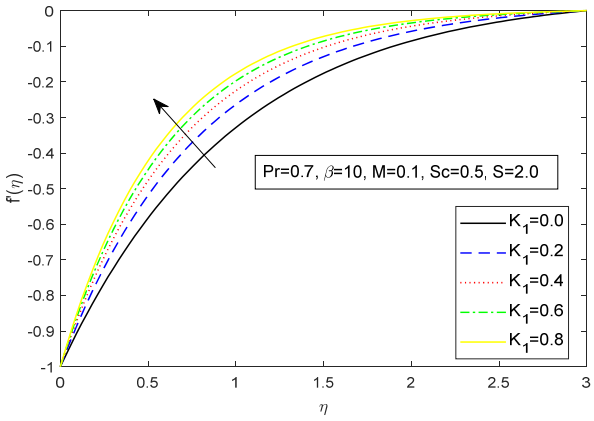

Figure 3. Velocity profile for K_1

Figure 3 portrays the velocity profile for diverse values of porosity parameter (K_1). Here we have seen that with enhancement of K_1, the velocity profile increases. As K_1 grows, the fluid has a larger area to move, which causes its velocity to rise. Figure 4 displays the thermal profile for various values of Prandtl number (Pr). From the figure it is clear that with rise in Pr, the thermal profile decreases. As Pr increases, the temperature drops. The thickness of the thermal boundary layer decreases with an increase in Prandtl number. The ratio of momentum diffusivity to heat diffusivity is known as the Prandtl number. Pr regulates the relative thickness of the thermal and momentum boundary layers in heat transfer issues. Figure 5 elucidates the variation of Schmidt number for species concentration profile. It is seen that the concentration falls, as Sc intensifies. The mass transfer rate rises with a higher Schmidt number, which causes the concentration profiles to fall. Figures 6 gives the impression that the fluid's velocity is accelerated by increasing Casson fluid parameter (β) values. Enhancement of β generally causes the fluid's motion to slow down since it increases the plastic dynamic viscosity. However, throughout the flow, an opposite behaviour is shown, and this is only possible

because geometry (shrinking sheet) is taken into consideration. Figure 7 and 8 presents the influence of Casson fluid parameter (β) on thermal, and species concentration profiles, respectively. It is evident from figure 7 that the fluid's temperature drops as it flows. Higher values of β may be physically attributed to improving the fluid's resistance and lessening the impacts of yield stress on the fluid, which causes the temperature pattern to slow down. Figure 9 represents the effect of suction parameter (S) on velocity profile. It is noted from the figure that velocity increases with enhancement of S, decreasing the thickness of the boundary layer.

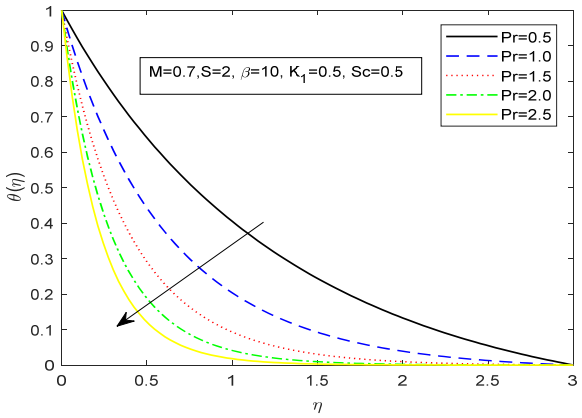

Figure 4. Temperature profile for Pr

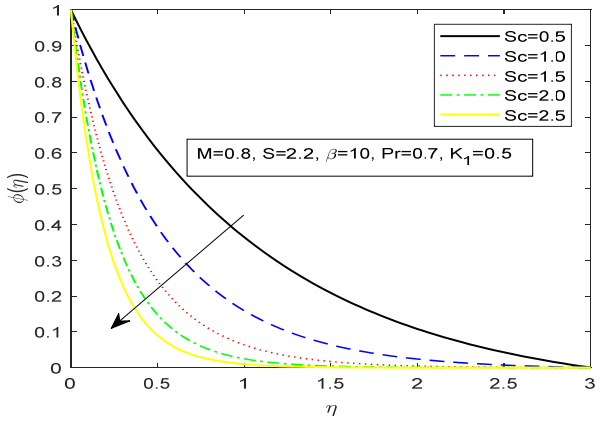

Figure 5. Concentration profile for Sc

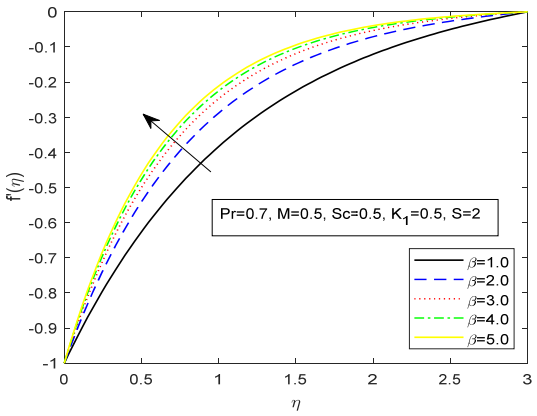

Figure 6. Velocity profile for β

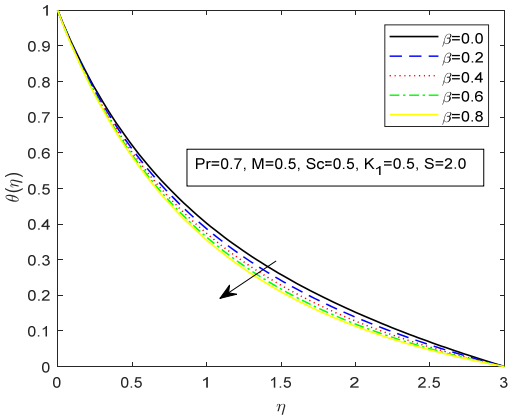

Figure7. Temperature profile for β

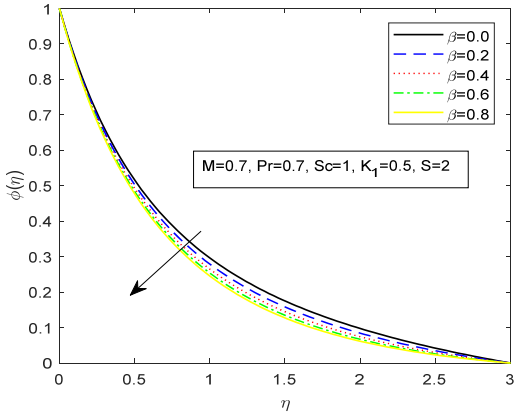

Figure 8. Concentration profile for β

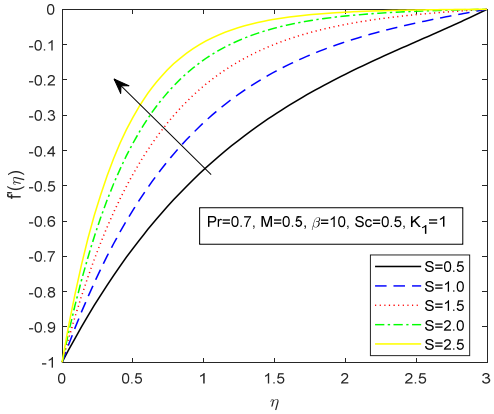

Figure 9. Velocity profile for S

4.1 VALIDATION OF RESULTS

To validate our numerical scheme, we compare our results with Bhattacharyya *et al.* [17], and they are found to be in good agreement with the result. (Table 1.)

In our experiment, Table 2 reflects the influence of the Magnetic parameter on the skin friction coefficient ($f''(0)$), Sherwood number ($-\phi'(0)$), and Nusselt number ($-\theta'(0)$). We have seen that Nusselt number, and Sherwood number exhibit a declining trend while skin friction increases as the Magnetic parameter increases. Table 3 elucidates the influence of porosity parameter (K_1) on the skin friction coefficient ($f''(0)$), Sherwood number ($-\phi'(0)$), and Nusselt number $\left(-\theta'(0)\right)$. From the table it is evident that as K_1 enhances, the skin friction coefficient trends enhancement on the other

hand the Nusselt number, and Sherwood number exhibit a declining trend. Table 4 depicts the impact of the Casson fluid variable on Sherwood number $(-\phi'(0))$, Nusselt number $\left(-\theta'(0)\right)$, and skin friction coefficient $f''(0)$ accordingly. We have identified that with an increase in the Casson fluid parameter, the skin friction coefficient experiences growth, but Nusselt number and Sherwood number experience a decline trend. Table 5 exhibits the influence of suction parameter (S) on the skin friction coefficient $(f''(0))$, Sherwood number $(-\phi'(0))$, and Nusselt number $(-\theta'(0))$. From the table, it is clear that as S increases, $f''(0)$ increases but Sherwood number and Nusselt number decrease.

Table 1. Numerical values of $f''(0)$, for Pr=0, Sc=0, K_1=0, M=0, β=1.

S	Bhattacharyya *et al.* [17]	Present Study
3.0	1.00000	1.0010
3.5	1.39039	1.3905
4.0	1.70711	1.7074
4.5	2.00000	2.0064
5.0	2.28078	2.2807

Table 2. Numeric data of Sherwood number, Nusselt number and Skin fraction for magnetic parameter (M)

Pr	Sc	S	K_1	β	M	Skin Friction	Nusselt number	Sherwood number
0.7	0.5	2.0	0.1	10	0.0	1.1803	-1.1622	-0.8682
					0.2	1.2272	-1.1667	-0.8715
					0.4	1.3473	-1.1778	-0.8794
					0.6	1.5070	-1.1914	-0.8892
					0.8	1.6846	-1.2049	-0.8990

Table 3. Numeric data of Sherwood number, Nusselt number and Skin fraction for porosity parameter (K_1)

Pr	Sc	S	M	β	K_1	Skin Friction	Nusselt number	Sherwood number
0.7	0.5	2.0	0.1	10	0.0	1.3380	-1.1770	-0.8789
					0.2	1.4999	-1.1908	-0.8888
					0.4	1.6317	-1.2010	-0.8962
					0.6	1.7452	-1.2092	-0.9021
					0.8	1.8461	-1.2160	-0.9070

Table 4. Numeric data of Sherwood number, Nusselt number and Skin fraction for Casson fluid parameter (β)

Pr	Sc	S	M	K_1	β	Skin Friction	Nusselt number	Sherwood number
0.7	0.5	2.0	0.5	0.1	0.0	0.3333	-1.0284	-0.7751
					0.2	0.3881	-1.0428	-0.7849
					0.4	0.4577	-1.0582	-0.7954
					0.6	0.5344	-1.0732	-0.8056
					0.8	0.6114	-1.0868	-0.8150

Table 5. Numeric data of Sherwood number, Nusselt number and Skin fraction for suction parameter (S)

Pr	Sc	β	M	K_1	S	Skin Friction	Nusselt number	Sherwood number
0.7	0.5	10	0.5	1	0.5	0.7730	-0.2918	-0.3046
					1.0	1.1238	-0.5451	-0.4759
					1.5	1.5187	-0.8662	-0.6819
					2.0	1.9376	-1.2218	-0.9112
					2.5	2.3694	-1.5896	-1.1548

5. CONCLUSION

We have numerically investigated the thermal and species concentration transmission of Casson fluid model over a shrinking surface. The governing equations are transformed into solvable ODEs, and bvp4c solver scheme is used to solve them. The key points of our study are listed below.

- As the magnetic parameter enhances, the motion of the Casson fluid increases.
- The porosity parameter enhances the velocity profile.
- With rises in Prandtl number, the temperature profile falls.
- The Casson fluid parameter is very important for controlling the fluid's temperature and concentration, which helps prevent damage to the system, as well as for helping the fluid develop its velocity.
- Schmit number retards the concentration profile.
- Suction phenomenon increases the velocity of the fluids.

ORCID

Rajesh Kumar Das, https://orcid.org/0000-0001-5190-3312; **Debasish Dey**, https://orcid.org/0000-0003-4215-6735

REFERENCES

[1] I.J. Grubka, and K.M. Bpbba, "Heat transfer characteristics of a continuous stretching surface with variable temperature," ASME J. Heat Transfer, **107**, 248-250 (1985). https://doi.org/10.1115/1.3247387
[2] W.H.H. Banks, "Similarity solutions of boundary layer equations for a stretching wall," J. Mech. Theor. Appl. **2**, 375-392 (1983).
[3] L.J. Crane, "Flow past a stretching plate," J. Appl. Math. Phys, (ZAMP), **21**, 645-647 (1970). https://doi.org/10.1007/BF01587695
[4] E. Magyari, and B. Keller, "Exact solution for self-similar boundary layer flows induced by permeable stretching walls," Eur. J. Mech. B/Fluids, **19**, 109-122 (2000). https://doi.org/10.1016/S0997-7546(00)00104-7
[5] S. Liao, and I. Pop, "On explicit analytic solutions of boundary layer equations about a flows in a porous medium or for a stretching wall," Int. J. Heat and Mass Transfer, **47**, 75-85 (2004). https://doi.org/10.1016/S0017-9310(03)00405-8
[6] C.Y. Wang, "Liquid film on an unsteady stretching sheet," Quart. Appl. Math. **48**, 601-610 (1990). https://doi.org/10.1090/qam/1079908
[7] M. Miklavcic, and C.Y. Wang, "Viscous flow due to a shrinking sheet," Quart. Appl. Math. **64**, 283-290 (2006). https://doi.org/10.1090/S0033-569X-06-01002-5
[8] T. Fang, and J. Zhang, "Closed-form exact solution of MHD viscous flow over a shrinking sheet," Commun. Nonlinear Sci. Num. Simulat. **14**, 2853–2857 (2009). https://doi.org/10.1016/j.cnsns.2008.10.005
[9] C.S.K. Raju, G. Neeraja, P.A. Dinesh, K. Vidya, and B.R. Kumar, "MHD Casson fluid in a suspension of convective conditions and cross diffusion across a surface of paraboloid of revolution," Alexandria Eng. J. **57**(4), 3615-3622 (2018). https://doi.org/10.1016/j.aej.2017.11.022
[10] M. Prameela, K. Gangadhar, and G.J. Reddy, "MHD free convective non-Newtonian Casson fluid flow over an oscillating vertical plate," Partial Differ. Equ. Appl. Math. **5**, 100366 (2022). https://doi.org/10.1016/j.padiff.2022.100366
[11] M.V. Krishna, "Chemical reaction, heat absorption and Newtonian heating on MHD free convective Casson hybrid nanofluids past an infinite oscillating vertical porous plate," Int. Commun. Heat Mass Transf. **138**, 106327 (2022). https://doi.org/10.1016/j.icheatmasstransfer.2022.106327
[12] M.S. Aghighi, A. Ammar, and H. Masoumi, "Double-diffusive natural convection of Casson fluids in an enclosure," Int. J. Mech. Sci. **236**, 107754 (2022). https://doi.org/10.1016/j.ijmecsci.2022.107754
[13] F. Hussain, M. Nazeer, M. Altanji, A. Saleem, and M.M. Ghafar, "Thermal analysis of Casson rheological fluid with gold nanoparticles under the impact of gravitational and magnetic forces," Case Stud. Therm. Eng. **28**, 101433 (2021). https://doi.org/10.1016/j.csite.2021.101433
[14] P.P. Humane, V.S. Patil, A.B. Patil, MD. Shamshuddin, and G.R. Rajput, "Dynamics of multiple slip boundaries effect on MHD Casson-Williamson double-diffusive nanofluid flow past an inclined magnetic stretching sheet," Proc. Inst. Mech. Eng. Part E: J. Process Mech. Eng. **236**(5), (2022). https://doi.org/10.1177/09544089221078153
[15] M. Awais, T. Salahuddin, and S. Muhammad, "Evaluating the thermo-physical characteristics of non-Newtonian Casson fluid with enthalpy change," Thermal Science and Engineering Progress, **42**, 101948 (2023). https://doi.org/10.1016/j.tsep.2023.101948
[16] E.N. Maraj, U. Faizan, and S. Shaiq, "Influence of joule heating and partial slip on casson nanofluid transport past a nonlinear stretching planar sheet," in: *International Conference on Applied and Engineering Mathematics, ICAEM*, (Taxila, Pakistan, 2019), pp.31-36. https://doi.org/10.1109/ICAEM.2019.8853731
[17] K. Bhattacharyya, M.S. Uddin, and G.C. Layek, "Exact solution for thermal boundary layer in casson fluid flow over permeable shrinking sheet with variable wall temperature and thermal radiation," Alexandria Engineering Journal, **55**, 1703-1712 (2016). https://doi.org/10.1016/j.aej.2016.03.010
[18] D. Dey, and B. Chutia, "Dusty nanofluid flow with bioconvection past a vertical stretching surface," **34**(6), 375-380 (2022). Journal of King Saud University- Engineering Sciences. https://doi.org/10.1016/j.jksues.2020.11.001
[19] D. Dey, and R. Borah, "Stability analysis on dual solutions of second-grade fluid flow with heat and mass transfers over a stretching sheet," *I*nternational Journal of Thermofluid Science and Technology, **8**(2), 080203 (2021). https://doi.org/10.36963/IJTST.2021080203
[20] D. Dey, and B. Chutia, "Modelling of multi-phase fluid flow with volume fraction past a permeable stretching vertical cylinder and its numerical study," Latin American Applied Research, **51**(3), 165-171 (2021). https://doi.org/10.52292/j.laar.2021.604
[21] Y. Khan, A. Hussain, and N. Faraz, "Unsteady linear viscoelastic fluid model over a stretching/shrinking sheet in the region of stagnation point flows," Sci. Iran. **19**, 1541–1549 (2012). https://doi.org/10.1016/j.scient.2012.10.019
[22] T. Hayat, T. Javed, and M. Sajid, "Analytic solution for MHD rotating flow of a second grade fluid over a shrinking surface," Phys. Lett. A, **372**, 3264–3273 (2008). https://doi.org/10.1016/j.physleta.2008.01.069
[23] T. Hayat, Z. Abbas, and N. Ali, "MHD flow and mass transfer of a upper-convected Maxwell fluid past a porous shrinking sheet with chemical reaction species," Phys. Lett. A, **372**, 4698–4704 (2008). https://doi.org/10.1016/j.physleta.2008.05.006
[24] T. Hayat, S. Iram, T. Javed, and S. Asghar, "Shrinking flow of second grade fluid in a rotating frame: an analytic solution," Commun. Nonlinear Sci. Num. Simul. **15**, 2932–2941 (2010). https://doi.org/10.1016/j.cnsns.2009.11.030
[25] G.R. Rajput, M.D. Shamshuddin, Sulyman, and O. Salawu, "Thermosolutal convective non-Newtonian radiative Casson fluid transport over a vertical plate propagated by Arrhenius kinetics with heat source/sink," Heat Transfer, **50**(3), 2829-2848 (2021). https://doi.org/10.1002/htj.22008
[26] M.D. Shamshuddin, and W. Ibrahim, "Finite element numerical technique for magneto-micropolar nanofluid flow filled with chemically reactive Casson fluid between parallel plates subjected to rotatory system with electrical and Hall currents," Int. J. Model. Simul. **42**(6), 985-1004 (2022). https://doi.org/10.1080/02286203.2021.2012634
[27] W. Alghamdi, T. Gul, M. Nullah, A. Rehman, S. Nasir, A. Saeed, and E. Bonyah, "Boundary layer stagnation point flow of the casson hybrid nanofluid over an unsteady stretching surface," AIP Advances, **11**, 015016 (2020). https://doi.org/10.1063/5.0036232
[28] D. Dey, and R. Borah, "Dual solutions of boundary layer flow with heat and mass transfers over an exponentially shrinking cylinder: stability analysis," Latin American Applied Research, **50**(4), 247–253 (2020). https://doi.org/10.52292/j.laar.2020.535
[29] Z. Shah, P. Kumam, and W. Deebani, "Radiative MHD casson nanofluid flow with activation energy and chemical reaction over past nonlinearly stretching surface through entropy generation," Scientific Reports, **10**(1), 4402 (2020). https://doi.org/10.1038/s41598-020-61125-9

[30] S. Nadeem, R. Mehmood, and N.S. Akbar, "Nanoparticle analysis for non-orthogonal stagnation point flow of a third order fluid towards a stretching surface," J. Comput. Theor. Nanosci. **10**, 2737–2747 (2013). https://doi.org/10.1166/jctn.2013.3274
[31] S. Nadeem, R.U. Haq, Z.H. Khan, "Numerical study of MHD boundary layer flow of a Maxwell fluid past a stretching sheet in the presence of nanoparticles," J. Taiwan Inst. Chem. Eng. **45**, 121–126 (2014). https://doi.org/10.1016/j.jtice.2013.04.006
[32] H. Rosali, A. Ishak, and I. Pop, "Micropolar fluid flow towards a stretching/shrinking sheet in a porous medium with suction," Int. Commun. Heat Mass Transf. **39**, 826–829 (2012). https://doi.org/10.1016/j.icheatmasstransfer.2012.04.008
[33] N.A. Yacob, and A. Ishak, "Micropolar fluid flow over a shrinking sheet," Meccanica, **47**, 293–299 (2012). https://doi.org/10.1007/s11012-011-9439-8
[34] N.A. Yacob, A. Ishak, and I. Pop, "Melting heat transfer in boundary layer stagnation-point flow towards a stretching/shrinking sheet in a micropolar fluid," Comput. Fluids, **47**, 16–21 (2011). https://doi.org/10.1016/j.compfluid.2011.01.040
[35] A. Ishak, Y.Y. Lok, and I. Pop, "Non-Newtonian power-law fluid flow past a shrinking sheet with suction," Chem. Eng. Commun. **199**, 142–150 (2012). https://doi.org/10.1080/00986445.2011.578696
[36] A. Ishak, Y.Y. Lok, and I. Pop, "Stagnation-point flow over a shrinking sheet in a micropolar fluid," Chem. Eng. Commun. **197**, 1417–1427 (2010). https://doi.org/10.1080/00986441003626169
[37] D. Dey, R. Borah, and A.S. Khound, "Stability analysis on dual solutions of MHD Casson fluid flow with thermal and chemical reaction over a permeable elongating sheet," Heat Transfer, **51**(4), 3401-3417 (2022). https://doi.org/10.1002/htj.22456
[38] T. Sarkar, S. Reza-E-Rabbi, S.M. Arifuzzaman, R. Ahmed, M.S. Khan, and S.F. Ahmmed, "MHD radiative flow of Casson and Williamson nanofluids over an inclined cylindrical surface with chemical reaction effects," Int. J. Heat Technol. **37**, 1117-1126 (2019). https://doi.org/10.18280/ijht.370421
[39] K. Bhattacharyya, T. Hayat, and A. Ahmed, "Analytic solution for magnetohydrodynamic boundary layer flow of Casson fluid over a stretching/shrinking sheet with wall mass transfer," Chin. Phys. B, **22**(2), 024702 (2013). https://doi.org/10.1088/1674-1056/22/2/024702
[40] D. Dey, R.K. Das, R. Borah, "A Simulation of Nanofluid Flow with Variable Viscosity and Thermal Conductivity Over a Vertical Stretching Surface," in: *Emerging Technologies in Data Mining and Information Security. Lecture Notes in Networks and Systems*, vol. 491, edited by P. Dutta, S. Chakrabarti, A. Bhattacharya, S. Dutta, V. Piuri, (Springer, Singapore, 2023). https://doi.org/10.1007/978-981-19-4193-1_18
[41] S. Pramanik, "Casson Fluid Flow and Heat Transfer past an Exponentially Porous Stretching Sheet in Presence of Thermal Radiation," Ain Shams Engineering Journal, **5**(1), 205-212 (2014). https://doi.org/10.1016/j.asej.2013.05.003
[42] A.S. Oke, W.N. Mutuku, M. Kimathi, and I.L. Animasaun, "Insight into the dynamics of non-newtonian casson fluid over a rotating non-uniform surface subject to coriolis force," Nonlinear Engineering, **9**(1), 398-411 (2020). https://doi.org/10.1515/nleng-2020-0025
[43] D. Dey, and M. Hazarika, "Entropy generation of hydro-magnetic stagnation point flow of micropolar fluid with energy transfer under the effect of uniform suction / injection," Latin American Applied Research, **50**(3), 209–214 (2020). https://doi.org/10.52292/j.laar.2020.206

ПОТІК РІДИНИ КАССОНА ПОВЗ ПОВЕРХНІ, ЩО СТИСКУЄТЬСЯ, З ТЕПЛО-ТА МАСОПЕРЕНОСОМ

Раджеш Кумар Дас[a], Дебасіш Дей[b]
[a]Департамент математики, Пандіт Діндаял Упадхьяя Адарша Махавідьялайя Амджонга, Гоалпара, Індія
[b]Департамент математики, Університет Дібругарх, Дібругарх, Індія

У цьому дослідженні чисельно досліджено поведінку тепло- та масопередачі потоку рідини Кассона повз пористий лист що стискається за наявності магнітного поля, теплового випромінювання та всмоктування або видування на поверхні. Застосовуючи відповідні перетворення подібності, основні часткові нелінійні диференціальні рівняння маси, потоку та теплопередачі перетворюються на звичайні диференціальні рівняння, які потім можна розв'язувати чисельно за допомогою схеми MATLAB bvp4c. Ми проаналізували та графічно показали вплив кількох безрозмірних керуючих факторів на профілі температури, концентрації та швидкості. Крім того, досліджено та зведено в таблиці тертя Шервуда, Нуссельта та Скіна для рідин Кассона. Результати поточного дослідження щодо рідини Кессона демонструють значну узгодженість із попередніми дослідженнями за конкретних обставин.

Ключові слова: *рідина Кассона; тепломасообмін; проникність; МГД; лист що стискається*